https://doi.org/10.5194/cp-2019-165
Preprint. Discussion started: 23 January 2020

Climate of the Past Discussions

A multi-model CMIP6 study of Arctic sea ice at 127 ka: Sea ice data compilation and model differences

Masa Kageyama[1,*], Louise C. Sime[2,*], Marie Sicard[1,*], Maria-Vittoria Guarino[2,*], Anne de Vernal[3], David Schroeder[4], Ruediger Stein[5], Irene Malmierca-Vallet[2], Ayako Abe-Ouchi[6], Cecilia Bitz[7], Pascale Braconnot[1], Esther Brady[8], Matthew A. Chamberlain[9], Danny Feltham[4], Chuncheng Guo[10], Gerrit Lohmann[5], Katrin Meissner[11], Laurie Menviel[11], Polina Morozova[12], Kerim H. Nisancioglu[13,14], Bette Otto-Bliesner[8], Ryouta O'ishi[6], Sam Sherriff-Tadano[6], Julienne Stroeve[15], Xiaoxu Shi[5], Bo Sun[16], Evgeny Volodin[17], Nicholas Yeung[11], Qiong Zhang[18], Zhongshi Zhang[19,10], and Tilo Ziehn[20]

[1]Laboratoire des Sciences du Climat et de l'Environnement, Institut Pierre Simon Laplace, Université Paris-Saclay, 91191 Gif-sur-Yvette Cedex, France
[2]British Antarctic Survey, Cambridge, UK
[3]Departement des sciences de la Terre et de l'atmosphere, Universite du Quebec, Montreal, Canada
[4]Department of Meteorology, University of Reading, Reading, UK
[5]Alfred Wegener Institute, Bremerhaven, Germany
[6]The University of Tokyo, Japan
[7]Department of Atmospheric Sciences, University of Washington, US
[8]National Center for Atmospheric Research, Boulder, US
[9]CSIRO Oceans and Atmosphere, Hobart, TAS, Australia
[10]NORCE Norwegian Research Centre, Bjerknes Centre for Climate Research, Bergen, Norway
[11]Climate Change Research Centre, The University of New South Wales, Sydney, Australia
[12]Institute of Geography, Russian Academy of Science, Moscow, Russia
[13]Department of Earth Science, University of Bergen, Bjerknes Centre for Climate Research, Allégaten 41, 5007, Bergen, Norway
[14]Centre for Earth Evolution and Dynamics, University of Oslo, Oslo, Norway
[15]University College London, UK
[16]Nanjing University of Information Science and Technology, Nanjing, China
[17]Institute of Numerical Mathematics, Russian Academy of Sciences, Moscow, Russia
[18]Department of Physical Geography, Stockholm University, Stockholm, Sweden
[19]Department of Atmospheric Science, School of Environmental Studies, China University of Geoscience (Wuhan), Wuhan, China
[20]CSIRO Oceans and Atmosphere, Aspendale, VIC, Australia
[*]The first four authors equally contributed to the manuscript

Correspondence: Masa Kageyama (Masa.Kageyama@lsce.ipsl.fr)

https://doi.org/10.5194/cp-2019-165
Preprint. Discussion started: 23 January 2020

Climate of the Past Discussions

Abstract. The Last interglacial (LIG) is a period with increased summer insolation at high northern latitudes, which results in strong changes in the terrestrial and marine cryosphere. Understanding the mechanisms for this response via climate modelling and comparing the models' representation of climate reconstructions is one of the objectives set up by the Paleoclimate Modelling Intercomparison Project for its contribution to the sixth phase of the Coupled Model Intercomparison Project. Here we analyse the results from 12 climate models in terms of Arctic sea ice. The mean pre-industrial to LIG reduction in minimum sea ice area (SIA) reaches 59% (multi-model mean LIG area is 2.21 mill. km^2, compared to 5.85 mill. km^2 for the PI), and the range of model results for LIG minimum sea ice area (from 0.02 to 5.65 mill. km^2) is larger than for PI (from 4.10 to 8.30 mill. km^2). On the other hand there is little change for the maximum sea ice area (which is 12 mill. km^2 for both the PI and the LIG, with a standard deviation of 1.04 mill. km^2 for PI and 1.21 mill. km^2 for LIG). To evaluate the model results we synthesize LIG sea ice data from marine cores collected in the Arctic Ocean, Nordic Seas and northern North Atlantic. South of 78°N in the Atlantic and Nordic seas the LIG was seasonally ice-free. North of 78 °N there are some discrepancies between sea-ice reconstructions based on dinocysts/foraminifers/ostracods and IP25: some sites have both seasonal and perennial interpretations based on the same core, but different indicators. Because of the conflicting interpretations it is not possible for any one model to match every data point in our data synthesis, or say whether the Arctic was seasonally ice-free. Drivers for the inter-model differences are: different phasing of the up and down short-wave anomalies over the Arctic ocean, associated with differences in model albedo; possible cloud property differences, in terms of optical depth; LIG ocean circulation changes which occur for some, but not all, LIG simulations. Finally we note that inter-comparisons between the LIG simulations, and simulations with moderate CO2 increase (during the transition to high CO2 levels), may yield insight into likely 21C Arctic sea ice changes using these LIG simulations.

https://doi.org/10.5194/cp-2019-165
Preprint. Discussion started: 23 January 2020

Climate of the Past Discussions

1 Introduction

The Last Interglacial (LIG) was the last time global temperature was substantially higher than the preindustrial, in particular at high northern latitudes. It is important in helping us understand warm climates sea ice and climate dynamics (Otto-Bliesner et al., 2013; Capron et al., 2017; Otto-Bliesner et al., 2017; Fischer et al., 2018). Stronger LIG spring and summertime insolation contributed to this warmth, as well as feedbacks amplifying the initial insolation signal, in particular feedbacks related to the marine and land cryosphere. Previous climate model simulations of the LIG, forced by appropriate greenhouse gas (GHG) and orbital changes, have failed to capture the observed high temperatures at higher latitudes (Malmierca-Vallet et al., 2018; Masson-Delmotte et al., 2011; Otto-Bliesner et al., 2013; Lunt *et al.*, 2013). Models used during the previous Coupled Model Intercomparison Project 5 (CMIP5) disagree on the magnitude of Arctic sea ice retreat during the LIG: the diversity of sea ice behaviour across models was linked to the spread in simulated surface temperatures and in the magnitude of the polar amplification (Otto-Bliesner et al., 2013; Lunt *et al.*, 2013; IPCC, 2013). However it was difficult to compare some of the LIG simulations because they were not all run using identical protocol. These studies thus highlighted the need of a systematic approach to study the role of Arctic sea ice changes during the LIG.

Coupled Model Intercomparison Projects (CMIPs) coordinate and design climate model protocols for the past, present and future climates, and have become an indispensable tool to facilitate our understanding of climate change (IPCC, 2007, 2013; Eyring et al., 2016). The Paleoclimate Model Intercomparison Project 4 (PMIP4) is one of the individual Model Intercomparison Projects which is taking part in CMIP6 (Kageyama et al., 2018). Within this framework, a common experimental protocol for Last Interglacial (LIG) climate simulation was developed by Otto-Bliesner et al. (2017). CMIP models differ among each other in their physical formulation, numerical discretization and code implementation. However this CMIP6-PMIP4 LIG standard protocol facilitates model inter-comparison work.

Alongside a previous lack of a common experimental protocol, our ability to evalutate CMIP models has previously been hindered by difficulties in determining LIG sea ice extent from marine core evidence (*e.g.* Otto-Bliesner et al., 2013; Sime et al., 2013; Malmierca-Vallet et al., 2018; Stein et al., 2017). Planktonic foraminifers representative of subpolar, seasonally open waters lived in the central part of the Arctic Ocean. These foraminifers suggest that the LIG Arctic Ocean was free of summer sea ice (Nørgaard-Pedersen et al., 2007; Adler et al., 2009). Microfauna found in LIG marine sediments recovered from boreholes on the Beaufort Sea Shelf seem to likewise support this idea; these indicate that more saline Atlantic water was present on the Beaufort Shelf, suggesting a lack of perennial Arctic sea ice during some part of the LIG (Brigham-Grette and Hopkins, 1995). Ostracodes from the Lomonosov and Mendeleyev Ridges and Morris Jesup Rise suggest minimum sea ice cover during the peak of the LIG (Cronin et al., 2010). Together this set of observations suggests an ice-free (summer sea ice free) Arctic during some part of the LIG. On the other hand, a reconstruction of LIG Arctic sea ice changes made by combining terrestrial and open-water phytoplankton biomarkers with the sea ice proxy IP25 (a carbon-25 highly-branched isoprenoid lipid) suggest that while a significant reduction of LIG sea ice occurred across the Barents Sea continental margin, the central part of the LIG Arctic Ocean remained ice covered during summer (Stein et al., 2017). Stein *et al.* (2017) thus may support the presence of sea ice in the Central Arctic throughout the LIG. However, for conditions of perennial sea ice or close

https://doi.org/10.5194/cp-2019-165
Preprint. Discussion started: 23 January 2020


Climate of the Past Discussions

to perennial sea ice, the association of low (or null) amounts of IP25 and phytoplankton markers is considered somewhat less robust compared with the other IP25 evidence (Belt, 2018). Interestingly though, despite the tendency for the marine evidence side to suggest low, or possibly even ice-free, conditions in LIG summer in the high Arctic, no previous coupled climate models have simulated an ice-free Arctic during the LIG (Otto-Bliesner et al., 2006; Lunt *et al.*, 2013; Otto-Bliesner et al., 2013; Stein et al., 2017).

Here we address the question of LIG Arctic sea ice by providing a new marine core synthesis. Additionally, the CMIP6-PMIP4 LIG experimental protocol developed by Otto-Bliesner et al. (2017) provides the systematic framework to enable us examine the question of the simulation of LIG Arctic sea ice using a multi-model approach. This is important given the current level of interest in the ability of climate models to accurately represent key Arctic climate processes during warm periods, including sea ice formation and melting. We compare the LIG Arctic sea ice simulated by each model against our new data synthesis, and investigate why different models show different Arctic sea ice behaviour.

2 Materials and methods

2.1 Current Arctic sea ice

Our main objective is to investigate LIG sea-ice. However, a quick assessment of the sea ice simulated in the reference state, i.e. the *piControl* experiment (PI) was necessary. In the absence of extensive sea ice data for the PI period, we used data for a recent period before the current sea ice cover significant decrease. We used the NOAA Optimum Interpolation version 2 data (Reynolds et al., 2002) for the period 1982 to 2001. The sea-ice data in this data set is obtained from different satellite and in-situ observations. We have used the monthly time series, at a resolution of 1° . This data set is termed 'NOAA_OI_v2' in the rest of this document.

2.2 Marine records of LIG Arctic sea ice

We focus here on records of sea ice from marine cores. Table 1 provides a summary of LIG sea ice information and data obtained from marine sediment cores collected in the Arctic Ocean, Nordic Seas and northern North Atlantic. South of 78°N, the records show ice-free conditions. Most of these sea ice records are derived from quantitative estimates of sea-surface parameters based on dinoflagellate cysts (dinocysts). North of 78°N the sea-ice related records are rare and different types of indicators were used. In addition to dinocysts, the records are based on biomarkers linked to phototrophic productivity in sea ice and on foraminifers and ostracods that both provide indication on water properties and indirectly on sea ice (de Vernal et al., 2013b). Between 78 and 87°N , the faunal data have been interpreted as indicating densely seasonal sea-ice cover conditions during the LIG.

https://doi.org/10.5194/cp-2019-165
Preprint. Discussion started: 23 January 2020

Climate of the Past Discussions

Table 1: Marine core records of Arctic sea ice from MIS5e. The references indicated for the dinocyst reconstructions are those for the initial core, the reconstruction itself follows de Vernal et al. (2013a, b, 2019) (*c.f.* main text for details).

Latitude (°N)	Longitude (°E)	Sea-ice indicator	Core name	Reference	Sea ice cover months		Annual mean SIC	
					Min	Max	Min	Max
87.08	144.77	Ostracode faunas	Oden96/12-1pc	Cronin et al. (2010)	3	11	0.15	0.95
85.32	-14	IP25	PS2200-5	Stein et al. (2017)	9	12	0.15	0.95
85.32	-14	Ostracode faunas	PS2200-5	Cronin et al. (2010)	3	11	0.15	0.95
85.14	-171.43	IP25	PS51/38-3	Stein et al. (2017)	9	12	0.15	0.95
84.81	-74.26	Subpolar foraminifers	GreenICE (core 11)	Nørgaard-Pedersen et al. (2007)	3	11	0.15	0.95
81.92	13.83	IP25	PS92/039-2	Kremer et al. (2018b)	3	12	0.3	0.95
81.54	30.17	Dinocysts	PS2138	Matthiessen et al. (2001)	1	6	0.15	0.5
81.54	30.59	IP25	PS2138-2	Stein et al. (2017)	6	12	0.15	0.95
81.19	140.04	IP25	PS2757-8	Stein et al. (2017)	9	12	0.15	0.95
79.59	-172.50	Subpolar foraminifers	HLY0503-8JPC	Adler et al. (2009)	3	11	0.15	0.95
79.32	-178.07	Ostracode faunas	NP26-32	Cronin et al. (2010)	3	11	0.15	0.95
79.20	4.67	IP25	PS93/006-1	Kremer et al. (2018a)	3	9	0.3	0.6
78.98	-178.15	Ostracode faunas	NP26-5	Cronin et al. (2010)	3	11	0.15	0.95
76.85	8.36	Dinocysts	M23455-3	Van Nieuwenhove et al. (2011)	0	1	0	0.15
70.01	-12.43	Dinocysts	M23352	Bauch and Andruleit (2013)	0	1	0	0.15
69.49	-17.12	Dinocysts	PS1247	N. Van Nieuwenhove	0	2	0	0.2

https://doi.org/10.5194/cp-2019-165
Preprint. Discussion started: 23 January 2020

67.77	5.92	Dinocysts	M23323	???	0	1	0	0.15
67.09	2.91	Dinocysts	M23071	Van Nieuwenhove et al. (2008); Van Nieuwenhove and Bauch (2008)	0	1	0	0.15
60.58	-22.07	Dinocysts	MD95-2014	Eynaud (1999)	0	0	0	0
58.77	-25.95	Dinocysts	MD95-2015	Eynaud et al. (2004)	0	0	0	0
58.21	-48.37	Dinocysts	HU90-013-13P	Hillaire-Marcel et al. (2001); de Vernal and Hillaire-Marcel (2008)	0	1	0	0.15
55.47	-14.67	Dinocysts	MD95-2004	Van Nieuwenhove et al. (2011)	0	0	0	0
53.33	-45.26	Dinocysts	HU91-045-91	A. de Vernal	0	1	0	0.15
53.06	-33.53	Dinocysts	IODP1304	A. de Vernal and B. Fréchette	0	1	0	0.15
50.17	-45.63	Dinocysts	IODP1302/1303	A. de Vernal and B. Fréchette	0	1	0	0.15
46.83	-9.52	Dinocysts	MD03-2692	Penaud et al. (2008)	0	0	0	0.15
37.80	-10.17	Dinocysts	MD95-2042	Eynaud et al. (2000)	0	0	0	0

Among sea-ice cover indicators, dinocyst assemblages have been used as quantitative proxy based on the application of the modern analogue technique applied to a standardized reference modern data base developed from surface sediment samples collected at middle to high latitudes of the Northern Hemisphere of the Northern Hemisphere (de Vernal et al., 2005; de Vernal et al., 2005b, 2013b, 2019). The sea-ice estimates from dinocysts used here are from different studies (see references in Table 1) and the new database including 71 taxa and 1968 stations (de Vernal et al., 2019). The reference sea ice data used for calibration are the monthly 1955-2012 average of the National Snow and Ice Data Center NSIDC: (Walsh et al., 2016). The results are expressed in term of annual mean of sea-ice cover concentration or as the number of months with >50% of sea-ice. The error of prediction for sea-ice concentration is ±12%.

Records of sea ice changes obtained by combining terrestrial and open-water phytoplankton biomarkers with the sea ice proxy IP25 (a carbon-25 highly-branched isoprenoid lipid), or PIP25, suggest that while a significant reduction of LIG sea ice

https://doi.org/10.5194/cp-2019-165
Preprint. Discussion started: 23 January 2020


Climate of the Past Discussions

occurred across the Barents Sea continental margin, perennial sea ice cover may have existed. Stein et al. (2017) emphasis that PIP25 has to be interpreted very cautiously if biomarker concentration are very low (see also Belt (2018)). The productivity of algal material (ice and open water) must have been quite low that (almost) nothing reached the seafloor or is preserved in the sediments, and there must have been periods during the LIG when some open-water conditions occurred, since subpolar foraminifers and coccoliths were found in core PS51/038 and PS2200 (Stein et al., 2017). It is however unclear whether these periods equate to more than a month per year of open water (or seasonal ice conditions). This explains why some sites show both seasonal and perennial interpretations at the same site. The reader is referred to the original publications (Table 1) for more information on these data.

Alongside the different types of sea ice indicators, another possible reason for the discrepancy between the dinocysts/-foraminifers/ostracods and the PIP25 core data interpretations may lie in the definition of 'perennial sea ice cover'. This is because perennial does not automatically mean 100% sea ice cover, or a sea ice concentration (SIC) of 1.0. It means rather that there is some sea ice, but not necessarily 100%, over the core site throughout the year (*i.e.* the summer season is not totally ice-free). With this in mind, we take the most cautious common approach to quantifying LIG sea ice presence. On a monthly basis, we use a standard SIC 0.15 threshold for ice-covered, this means that the minimum annual mean SIC for perennial sea ice is 0.15 for records which have been interpreted as covered by perennial sea ice. Due to the presence of sea ice leads, or gaps in the ice, we assume a maximum SIC of 0.95. Using this approach, it is not possible to reliably distinguish between seasonally and perennially covered areas using SIC annual mean. For this reason, it is more reliable to compare the number of months that a core site is covered, rather than using SIC annual mean data. For completeness, we do however provide both sets of data: minimum and maximum numbers of months of sea ice cover, and annual mean SIC numbers in Table 1.

A third factor is the spatial (area) definition of 'ice-free'. The Arctic is considered ice-free when, on any given day, the total area of sea ice is less than 1 million km^2. This means that some marine core sites could remain ice covered for the summer, but the Arctic would nevertheless remain technically ice-free.

Other new QUIGS (Quaternary Interglacials) PAGES-PMIP working group syntheses aredescribed in Otto-Bliesner et al., (in prep, companion paper to the present work), which updates LIG temperature and other LIG data synthesis.

2.3 CMIP6-PMIP4 Models

The last Coupled Model Intercomparison Project Phase 5 (CMIP5) collected climate simulations performed with 60 different numerical models by 26 research institutes around the world (IPCC, 2013). The follow-on CMIP6 archive, to be completed in 2020, is expected to gather model outputs from over 30 research institutes. Of these, currently twelve models have run the CMIP6-PMIP4 LIG simulation (Table 2). We present results here from all twelve of these models.

Table 2 provides an overview of the models used in this study. They are state-of-the-art coupled general circulation models (GCM) and Earth System Models (ESM) simulating the atmosphere, ocean, sea ice and land surface processes dynamics with a varying degree of complexity across them. These models have been developed for several years by individual institutes across the world and, in the context of CMIP6, are used in the same configuration to simulate seamlessly past, present and future climate.

https://doi.org/10.5194/cp-2019-165
Preprint. Discussion started: 23 January 2020

Climate of the Past Discussions
Open Access
EGU

Table 2 shows for each model: model denomination, physical core components, horizontal and vertical grid specifications, details on prescribed vs interactive boundary conditions, relative publication for an in-depth model description, and LIG simulation length (spin-up and production runs).

https://doi.org/10.5194/cp-2019-165
Preprint. Discussion started: 23 January 2020

Climate of the Past Discussions

Table 2: Overview of models that have run the CMIP6-PMIP4 LIG simulation. For each model, denomination, physical core components, horizontal and vertical grid specifications, details on prescribed vs interactive boundary conditions, reference publication and LIG simulation length is shown.

Model name	Physical core components	Model grid (i_lon X i_lat X z_lev)	Boundary Conditions	Reference publication	LIG simulation length (yrs)
ACCESS-ESM1-5	Atmosphere: UM Land: CABLE2.4 Ocean: MOM5 Sea Ice: CICE4.1	Atmosphere: 192x145 x L38 Ocean: 360x300 x L50	Vegetation: prescribed Aerosol: prescribed Ice-Sheet: prescribed	Ziehn et al. (2017)	Spin-up: 400 Production: 200
AWIESM2	Atmosphere: ECHAM6.3.04p1 Land: JSBACH 3.20 Ocean: FESOM 2 Sea Ice: FESOM 2	Atmosphere: 192x96 x L47 Ocean: unstructured grid 126858 nodes x L48	Vegetation: interactive Aerosol: prescribed Ice-Sheet: prescribed	Sidorenko et al. (2015)	Spin-up: 1000 Production: 100
CESM2	Atmosphere: CAM6 Land: CLM5 Ocean: POP2 Sea Ice: CICE5.1	Atmosphere: 288x192 x L32 Ocean: 320x384 x L60	Vegetation: prescribed Aerosol: Ice-Sheet:	Danabasoglu et al. (2019)	Spin-up: Production:
EC-Earth3	Atmosphere: IFS-cy36r4 Land: HTESSEL Ocean: NEMO3.6 Sea Ice: LIM3	Atmosphere: 512×256 x L91 Ocean: 362×292 x L75	Vegetation: prescribed Aerosol: prescribed Ice-Sheet: prescribed	Hazeleger et al. (2012)	Spin-up: 300 Production: 200
HadGEM3-GC3.1-LL	Atmosphere: MetUM-GA7.1 Land: JULES-GA7.1 Ocean: NEMO-GO6.0 Sea Ice: CICE-GSI8	Atmosphere: 192×144 x L85 Ocean: 360×330 x L75	Vegetation: prescribed Aerosol: Prescribed Ice-Sheet: prescribed	Williams et al. (2018)	Spin-up: 350 Production: 200
INM-CM4-8	Atmosphere: INM-AM4-8 Land: INM-LND1 Ocean: INM-OM5 Sea Ice: INM-ICE1	Atmosphere: 180x120 x L21 Ocean: 360x318 x L40	Vegetation: prescribed Aerosol: interactive Ice-Sheet: prescribed	Volodin et al. (2018)	Spin-up: 50 Production: 100

https://doi.org/10.5194/cp-2019-165
Preprint. Discussion started: 23 January 2020

IPSL-CM6A-LR	Atmosphere: LMDZ6 Land: ORCHIDEE Ocean: NEMO-OPA Sea Ice: NEMO-LIM3	Atmosphere: 144x143 x L79 Ocean: 362x332 x L75	Vegetation: prescribed PFTs, interactive phenology Aerosol: Prescribed PI values Ice-Sheet: prescribed	Boucher et al. (2019)	Spin-up: 300 Production: 200
LOVECLIM1.2	Atmosphere: Land: Ocean: Sea Ice:	Atmosphere: 64x32 x L3 Ocean: 120x65 x L20	Vegetation: interactive Aerosol: - Ice-Sheet: prescribed	Goosse et al. (2010)	Spin-up: Production:
MIROC-ES2L	Atmosphere: CCSR AGCM Land: MATSIRO6.0 +VISIT-e Ocean: COCO4.9 Sea Ice: COCO4.9	Atmosphere: 128x64 x L40 Ocean: 360x256 x L63	Vegetation: prescribed Aerosol: prescribed Ice-Sheet: prescribed	Hajima et al. (2019) Tatebe et al. (2018)	Spin-up: 1450 Production: 100
NESM3	Atmosphere: ECHAM6.3 Land: JS-BACH Ocean: NEMO3.4 Sea Ice: CICE4.1	Atmosphere: 192x96 x L47 Ocean: 384x362 x L46	Vegetation: Aerosol: Ice-Sheet:	Cao et al. (2018)	Spin-up: Production: 100
NorESM1-F	Atmosphere: CAM4 Land: CLM4 Ocean: MICOM Sea Ice: CICE4	Atmosphere: 144x96 x L26 Ocean: 360x384 x L53	Vegetation: prescribed, as PI Aerosol: prescribed, as PI Ice-Sheet: prescribed, as PI	Guo et al. (2019)	Spin-up: 500 Production: 200
NorESM2-LM	Atmosphere: CAM-OSLO Land: CLM Ocean: BLOM Sea Ice: CICE	Atmosphere: 144x96 x L32 Ocean: 360x384 x L53	Vegetation: as in PI Aerosol: as in PI Ice-Sheet: as in PI	Seland et al. (2019)	Spin-up: 300 Production: 200

130

2.4 PMIP4 LIG (*lig127k*) simulation protocol

Results shown here are from main Tier 1 LIG simulation, from the standard CMIP6-PMIP4 LIG experimental protocol (Otto-Bliesner et al., 2017). The prescribed LIG (*lig127k*) protocol differs from the CMIP6 Pre-industrial (PI) simulation protocol in astronomical parameters and the atmospheric trace GHG concentrations. LIG astronomical parameters are prescribed according
135 to orbital constants (Berger and Loutre, 1991), and atmospheric trace GHG concentrations are based on ice core measurements. See Table 3 for a summary from Otto-Bliesner et al. (2017). All other boundary conditions, including solar activity, ice sheets, aerosol emissions and etc., are identical to PI protocol.

https://doi.org/10.5194/cp-2019-165
Preprint. Discussion started: 23 January 2020

Climate of the Past Discussions

LIG simulation were initialized either from a previous LIG run, or from the standard CMIP6 protocol preindustrial simulations, using constant 1850 GHGs, ozone, solar, tropospheric aerosol, stratospheric volcanic aerosol and land use forcing.

Although PI and LIG spin-ups vary between the models, most model groups aimed to allowed the land and oceanic masses to attain approximate steady state *i.e.* to reach atmospheric equilibrium and to achieve an upper-oceanic equilibrium. LIG production runs are all between 100-200 years long, which is generally within the appropriate length for Arctic sea ice analysis (Guarino et al., 2019).

Table 3. Astronomical parameters and atmospheric trace gas concentrations used to force LIG and PI simulations.

Astronomical parameters	**LIG**	**PI**
Eccentricity	0.039378	0.016764
Obliquity	24.040°	23.459°
Perihelion-180°	275.41°	100.33°
Date of vernal equinox	March 21 at noon	March 21 at noon
Trace gases		
CO2	275 ppm	284.3 ppm
CH4	685 ppb	808.2 ppb
N2O	255 ppb	273 ppb

3 Results: simulated Arctic sea ice

Since all LIG production runs are at least 100 years in length, all model results are averaged over at least 100 years. We refer to the multi-model mean throughout as the MMM. Sea ice areas (SIAs) are calculated using a standard approach, *i.e.* by considering the area covered by sea ice whose fraction is larger than 0.15. The Arctic sea ice area is computed for latitudes higher than 60°N .

3.1 PI sea ice

For the present-day we have satellite and in-situ observations with which to evaluate the models. The use of present-day sea ice data implies that we might expect our PI sea ice MMM to be generally somewhat larger than the observed mean. Figure 2 shows the mean seasonal cycle of the Arctic sea-ice extent simulated for the PI and LIG alongside the observed Arctic sea-ice extent.

The summer minimum monthly MMM area for the PI is 5.85 ± 1.24 mill. km^2, compared to the observed 1981 to 2002 mean of 5.51 mill km^2. Interestingly this MMM PI area is a little larger than the 1981–2002 area. The majority of the simulations show a realistic representation of the geographical extent for the summer minimum (Figure 3), with eight out of twelve models showing a slightly smaller area compared to the present-day observations, and four showing an overestimated area. LOVECLIM and EC-Earth have clearly too much ice (Table 4). The other models generally exhibit realistic PI summer minimum

https://doi.org/10.5194/cp-2019-165
Preprint. Discussion started: 23 January 2020


Climate of the Past Discussions

ice conditions. The detail of the geographical distribution of sea ice for the models, the MMM and the NOAA_OI_v2 data sets (Fig. 3) confirms the results in terms of Arctic sea-ice extent. The large overestimation for LOVECLIM (Barents-Kara Seas and Nordic Seas) and EC-Earth (Nordic Seas) is also apparent. MIROC-ES2L performs rather poorly for the PI, with insufficient ice close to the continents. The other models are generally matching the 0.15 isoline from the NOAA_OI_v2 data set in a realistic manner. The winter maximum monthly MMM areas show little difference between the present day and PI simulated areas. The MMM PI area is 12.05 $\pm$ 2.23 mill km^2, compared to the observed 1981 to 2002 mean of 12.31 mill km^2. For both the summer and winter, the simulations and observations mostly agree on the month that the minimum and maximum are attained: July-August for the minimum ; and Jan-Feb for the maximum for every model (except NESM3, which is March; Table 4).

The comparison between the model results and NOAA_OI_v2 data sets as a function of latitude for PI (Figures 5a and 7) at the sites for which there are sea ice reconstructions for the LIG shows that nine of twelve models match the observations south of 70°N. Between 70 and 78°N, there tend to be a model-data mismatch: around seven model have issues with getting the months of sea ice correct in the Nordic Seas, near Greenland and the sea ice edge. North of this all the models get the months of perennial PI sea ice correct.

3.2 LIG sea ice

The models show a summer minimum monthly MMM area for the LIG of 2.39 $\pm$ 1.29 mill. km^2, and a winter monthly MMM area of 11.99 $\pm$ 1.21 mill. km^2. Thus there is a reduction in SIA in the MMM of 49% for the minimum summer month, but almost no change for the winter month MMM. Every model shows a reduction, often substantial, in summer sea ice between the PI and LIG.

Three models, of the thirteen, show the LIG Arctic with (or near) seasonally ice-free conditions *i.e.* very close to the ice-free threshold (of 1 mill. km^2). Of these three, only two realistically capture the PI Arctic: CESM2 and HadGEM3. CESM2 has 1.27 mill. km^2 during the LIG, whilst HadGEM3 is ice-free. There is a large amount of inter-model variability for the LIG during the summer (Figure 4 and Table 4).

For the winter only six of the twelve models show a (small) winter reduction in sea ice between the PI and LIG. All models therefore show a larger sea-ice area amplitude for LIG than for PI, and the range of model results is larger for LIG than for PI. The summer season, but also the seasons of sea ice growth and decay, are therefore key to understand the behaviour of LIG sea ice and the inter-model differences, as will be confirmed in Section 4.

3.3 LIG model-data comparison

We compare the model results to reconstructions in terms of three broad categories: perennial sea-ice cover, seasonal cover and ice free sites. To compute those, we consider the number of months, in the mean seasonal cycle, for which the sea ice fraction is larger than 0.15 and define perennial sea ice to have at least 9 months of coverage, ice free areas to have less than 3 month coverage, and seasonal sea ice cover otherwise. Because several of the marine cores have ambiguous interpretations, suggesting both perennial and seasonal sea ice at the same high Arctic sites, it is not possible to for any one model to match

https://doi.org/10.5194/cp-2019-165
Preprint. Discussion started: 23 January 2020

Climate of the Past Discussions

Table 4. Sea ice area (for sea ice fraction > 0.15) for the PI and LIG simulations. MMM stands for the multi-model mean, STD for the multi-model standard deviation.

	PI sea ice in 10^6 km^2		**LIG sea ice in 10^6 km^2**	
Model or dataset	minimum (month)	maximum (month)	minimum (month)	maximum (month)
NOAA_OI_v2	5.51 (8)	12.31 (2)	na	na
ACCESS	5.07 (8)	11.31 (2)	2.01 (7)	10.77 (2)
AWIESM2	5.10 (8)	10.83 (2)	3.10 (7)	10.65 (2)
CESM2	5.13 (8)	12.55 (2)	1.27 (7)	12.63 (2)
EC-Earth	7.32 (7)	12.72 (2)	3.00 (7)	11.34 (2)
HadGEM3	5.27 (7)	11.45 (2)	0.02 (7)	10.62 (2)
INMCM4-8	7.60 (7)	13.06 (1)	5.65 (7)	12.77 (2)
IPSLCM6	5.83 (7)	12.80 (2)	2.36 (7)	12.73 (2)
LOVECLIM	8.30 (7)	12.77 (1)	2.89 (7)	12.89 (2)
MIROC-ES2L	4.10 (7)	11.72 (2)	2.61 (7)	11.79 (2)
NESM3	5.03 (8)	14.49 (3)	1.35 (7)	14.98 (3)
NORESM1-F	4.81 (8)	11.35 (2)	2.23 (7)	11.57 (2)
NORESM2-LM	5.10 (8)	10.88 (2)	2.18 (7)	11.26 (2)
MMM	5.85 (7)	12.15 (2)	2.39 (7)	11.99 (2)
STD	1.24	1.04	1.29	1.21

every data point in Table 1. That said, the comparison between the PI and LIG results and PI and LIG sea ice data as a function of the latitude of the LIG data sites is remarkably similar for each individual model (Figure 5): the same models that struggle with realistically representing the sea ice cover duration (at a core site) in the PI tend also to struggle with it for the LIG. The main problem area in this core-site-by-core-site comparison remains the Nordic Seas, near to Greenland and the PI sea ice edge, between 70 and 78°N. In the high Arctic, north of 78°N the marine cores with dual interpretations means we cannot unambiguously (from the Table 1 dataset) identify which models are accurately capturing the LIG sea ice conditions. In fact, some models support the interpretation of perennial sea ice, while other support the one of some months during summer being ice free.

Figure 6 shows the geographical model-data match. From this, we see that it is more difficult for the models to realistically capture sea ice change over the near Greenland core sites, close to the sea ice edge. If we cross compare the observation-model match for each model for both the PI (Figure 7) and the LIG (Figure 6) then LOVECLIM and NESM3 have particular problem accurately capturing sea ice at the core site locations near Svalbard, whilst NORESM1-F does the best job of capturing the near Greenland, Nordic seas sea ice edge for both time periods. It is these Nordic Seas sea ice edge differences (over the Table 1 core sites) that make the difference between the simulation-data matches for each model.

https://doi.org/10.5194/cp-2019-165
Preprint. Discussion started: 23 January 2020


Climate of the Past Discussions

Farther north, in the high Arctic, the simulation-data agreement is perfect for the PI (and likewise for the ice-free Atlantic regions). But it is not possible, from Figure 6, to establish differences which occur for all models for the LIG. This is perhaps inevitable given that some marine cores have interpretations which suggest both perennial and seasonal sea ice at the same high Arctic sites. The marine core community may need to resolve this dinocyst/foraminifers/ostracod and the PIP25 core data interpretation discrepancy before establishing a most likely sea ice change from this data.

4 Discussion of model differences

Whilst we cannot yet definitely establish the most likely Arctic sea ice conditions during the LIG, we can investigate sea ice differences across models when we have sufficient model data. To can do this analysis for the three models for which we have sufficient data: CESM2, HadGEM3, and IPSLM6. These models each represent a distinct sea ice response to the LIG forcing, *i.e.* summer sea ice concentration less than 0.15 everywhere (HadGEM3), significant summer sea ice retreat with concentration less than 0.8 in central Arctic (CESM2), modest summer sea ice retreat with a small area with sea ice concentration close to 1 in Central Arctic (IPSLCM6).

Sea ice formation and melting can be affected by a large number of factors inherent the atmosphere and the ocean dynamics, alongside the representation of sea ice itself within the model (*i.e.* the type of sea ice scheme used). In coupled models it can be extremely difficult to identify the causes of essentially coupled-model behaviour. Nevertheless, we discuss the short-wave (SW) surface energy balance, ocean circulation, and comment on cloudiness and albedo changes.

4.1 Atmospheric energy budget differences

The atmospheric energy budget LIG – PI anomaly (Fig. 8) is negative in winter and strongly positive in summer, following the imposed insolation anomaly. These anomalies in total heat budget are dominated by the SW budget contribution from May to August. We split the SW budget into the SWdown and SWup contributions. The SWup flux anomaly shown on Fig. 8 is counted positive downward, which means that the total SW budget (in black) is the sum of the SWdn contribution (in red) and the SWup contribution (in blue). On this figure, a positive SWup anomaly means that the SWup is less intense at LIG than at PI, hence contributing to an increase in the net SW flux.

For all the models, the total heat budget anomaly is due to (i) an increased downward SW flux in spring resulting from the insolation forcing, and (ii) a decreased upward shortwave flux in summer, related to the decrease of the albedo due to the smaller sea-ice cover. During summer, this decrease in upward shortwave flux more than compensates the decrease in SWdn, which is maximum in August.

The summer anomaly reaches 80 W/m2 in June for HadGEM3, 60 W/m2 for IPSLCM6, 50 W/m2 for CESM2. The differences between the model results are due to a different phasing of the SWdn and SWup anomalies for HadGEM3, compared to the other two models: for HadGEM3, the two fluxes peak in June, while for CESM2 and IPSLCM6, the SWdn flux peaks in May and the SWup signal peaks in July, so that the anomaly in these fluxes partly compensate. HadGEM3 shows a larger net SW increase despite a SWdn anomaly which is smaller than for the other two models. On the other hand, HadGEM3's SWup

https://doi.org/10.5194/cp-2019-165
Preprint. Discussion started: 23 January 2020


Climate of the Past Discussions

component is stronger and always positive, which is different to the other two models which show a negative SWup contribution in April-May. These differences are associated with differences in albedo for the three models (Fig. 9). HadGEM3's sea ice and Arctic ocean albedos are always smaller than those simulated by IPSLCM6 and CESM2 and the difference is larger for LIG than for PI. The albedo simulated by HadGEM3 in May and June is particularly low compared to the two other models, which explains why the SWup component peaks earlier. The albedo LIG–PI anomalies over the whole Arctic show that the sea-ice albedo feedback is most effective in HadGEM3.

In terms of cloudiness, IPSLCM6 shows differences in the properties of clouds, in terms of optical depth, between PI and LIG, but this could not be investigated, due to a lack of data (thus far), for the other models. Thus we cannot tell if LIG–PI anomalies in SWdn fluxes, *i.e.* differences between HadGEM3's and CESM2 flux also have a contribution due to cloud changes.

4.2 Ocean circulation differences

Changes in Arctic sea ice related to ocean heat transport have been found for the CESM large ensemble (Auclair and Tremblay, 2018). The differences can then be amplified by the sea-ice albedo feedbacks. We check this in our models by calculating long-term means of the maximum meridional stream function at 26°N for the PI and LIG simulations. These are 19.5 and 18.7 for CESM2, 15.6 and 15.8 Sv for HadGEM3, and 12.9 and 10.4 for IPSLCM6. Thus, the CESM2 and HadGEM3 models exhibit an AMOC that is almost unchanged between PI and LIG, while in the IPSLCM6 model the AMOC weakens. This implies that a reduced northward oceanic heat transport could prevent sea ice loss in the central Arctic in some but not all models (see also Stein et al., 2017).

Some differences in the response of sea ice to LIG forcing therefore appear to be due either to differences in atmospheric response (HadGEM3 vs IPSL-CM6 and CESM2), similar to mechanisms found for current sea ice decline (*e.g.* He et al. (2019); Olonscheck et al. (2019)) or to changes in ocean heat transport (CESM2 vs IPSLCM6). But while AMOC changes partially explain the differences found between IPSL (more sea ice in central Arctic) and CESM2 and HadGEM3 (less sea ice in central Arctic), they do not explain differences between ice-free and ice-covered conditions in HadGEM3 and CESM2. Other factors which remain to be investigated include clouds and ocean heat uptake in the Arctic in the different models, for example, as a function of stratification.

4.3 Transient CO2 forced responses: LIG vs transient 1pctCO2

The LIG has higher insolation than PI at high northern latitudes during spring and summer, and less significant changes in winter insolation. This is distinct from the increased GHG which is the dominant forcing for future climates. However, since sea ice minimum occurs in summer, it is of interest to consider possible relationships between CMIP6 model responses for the LIG and those for the transient *1pctCO2* experiments. Seven models have the LIG, PI and *1pctCO2* simulations available. These include models with large, small and intermediate responses in sea-ice for the LIG.

Figure 10 suggests that there is indeed such a relationship between the summer sea-ice concentration decreases for LIG and the averages from years 50 to 70 of the transient 1pctCO2 simulations : the models which responds strongly at LIG also

https://doi.org/10.5194/cp-2019-165
Preprint. Discussion started: 23 January 2020


Climate of the Past Discussions

respond strongly for the 1pctCO2 forcing, and the model with the smallest response for LIG (INMCM4-8) has the smallest response to the 1pctCO2 forcing. The relationship shown in Figure 10 does not last for later periods in the 1pctCO2 runs, when the winter sea-ice is also affected by the increased greenhouse gas forcing. This implies inter-comparisons between the LIG simulation, and simulations with moderate CO2 increase (during the transition to high CO2 levels), should be investigated.

5 Conclusions

The Last Interglacial (LIG) was the last time global temperature was substantially higher than the preindustrial at high northern latitudes (Otto-Bliesner et al., 2013; Capron et al., 2017; Otto-Bliesner et al., 2017; Fischer et al., 2018). To help understand the role of Arctic sea ice in these changes, we present a new synthesis of LIG sea ice information using marine core data collected in the Arctic Ocean, Nordic Seas and northern North Atlantic - and compare this to PMIP4-LIG simulations.

Our synthesis shows that south of 78°N in the Atlantic and Nordic seas the LIG was definitely seasonally ice-free. These southern sea ice records are derived from quantitative estimates of sea-surface parameters based on dinoflagellate cysts (dinocysts). North of 78°N the sea-ice related records are more difficult to obtain and interpret. Some records here are based on biomarkers linked to phototrophic productivity in sea ice and on foraminifers and ostracods that both provide indication on water properties and indirectly on sea ice (de Vernal et al., 2013b). North of 78 °N, these faunal data have been interpreted as indicating densely seasonal sea-ice cover conditions during the LIG. However north of 78 °N records obtained by combining terrestrial and open-water phytoplankton biomarkers with the sea ice proxy IP25 (a carbon-25 highly-branched isoprenoid lipid), or PIP25, suggest that while a significant reduction of LIG sea ice occurred across the Barents Sea continental margin, perennial sea ice cover may have existed (Stein et al., 2017). It is unclear whether these periods equate to more than a month per year of open water (or seasonal ice-free conditions).

As a result of the discrepancy between the dinocysts/foraminifers/ostracods and the PIP25 core data interpretations, some sites in the synthesis have both seasonal and perennial interpretations based on the same core. Additionally, the definition of 'perennial sea ice cover' has previously been unclear. Perennial does not automatically mean a sea ice concentration of 1.0. To address this here we quantify LIG sea ice presence on a monthly basis, using a standard SIC 0.15 threshold for ice-covered. This means that the minimum annual mean SIC for perennial sea ice is 0.15 for records which have been interpreted as covered by perennial sea ice (which also implies open water). Thus the definitions of ice free and seasonal in the literature need to be treated with care. It is also noted that, the Arctic is considered ice-free when, on any given day, the total area of sea ice is less than 1 million km^2. This means that some marine core sites could remain ice covered for the summer, but the Arctic would nevertheless remain technically seasonally ice-free.

Model results from thirteen models show a multi model mean (MMM) summer SIA LIG of 2.39 $\pm$ 1.29 mill. km^2, and a winter monthly MMM area of 11.99 $\pm$ 1.21 mill. km^2. This is a a reduction in SIA of 59% for the minimum summer month between the PI and LIG, but almost no change for the winter month MMM. Every model shows a reduction, often substantial, in summer sea ice between the PI and LIG. For the winter only six of the thirteen models show a (small) winter reduction in sea ice between the PI and LIG. This reinforces that the key season for understanding LIG warming is the summer.

https://doi.org/10.5194/cp-2019-165
Preprint. Discussion started: 23 January 2020

Because several of the marine cores have conflicting interpretations it is not possible for any one model to match every data point in the data synthesis. In general, the same models that struggle with realistically representing the numbers of months of sea ice in the PI that struggle with the LIG. The main problem area for matching the core sites (with unambiguous interpretations) remains the Nordic Seas, near to Greenland and the PI sea ice edge, between 70 and 78°N. It is not possible, based on our synthesis, to identify which models are accurately capturing the LIG sea ice conditions in the high Arctic.

Whilst we show that we cannot establish which models accurately capture LIG Arctic sea ice, we do investigate sea ice differences across models. We find that the total heat LIG Arctic budget anomaly is due to (i) an increased downward SW flux in spring, due to the insolation forcing, and (ii) an decreased upward shortwave flux in summer, related to the decrease of the albedo due to the smaller sea-ice cover. During summer, this decrease in upward shortwave flux more than compensates the decrease in the SW down, which is maximum in August. Differences between the model results are due to a different phasing of the up and down SW anomalies in the different models, and are associated to the differences in model albedo.

Analysis of IPSLCM6, shows differences in the properties of clouds, in terms of optical depth, between PI and LIG. Further work is required to identify if this is also important for other models. Changes in Arctic sea ice may also be related to ocean heat transport. Here, we have shown that ocean circulation changes occur for some, but not all, LIG simulations. Other factors which remain to be investigated include clouds and ocean heat uptake in the Arctic in the different model.

Finally we note that there is an apparent relationship between the summer sea-ice areas simulated for the LIG and the ones averaged over years 50 to 70 of the transient 1pctCO2 simulations: the models which responds strongly to the LIG forcing also respond strongly for the 1pctCO2 forcing. This implies inter-comparisons between the LIG simulation, and simulations with moderate CO2 increase (during the transition to high CO2 levels), may yield insight into likely 21C Arctic sea ice changes from LIG simulations, especially if we achieve a less ambiguous characterisation of LIG sea ice from marine cores.

Data availability. The majority of the model simulations used in this study are available or will shortly be available on the Earth System Grid Federation (https://esgf-node.llnl.gov/), the data repository for CMIP6 simulations. All CMIP6 outputs are expected to be public by the end 2020. Data not yet public can be shared, under request, by the authors.

Author contributions. MK, LS, MS, MG are joint first authors for this manuscript. MK and LS planned the study, with other QUIGs members. MK and MS analysed all model simulations and produced all model figures. LS wrote the manuscript. MG contributed substantially to the first draft and compiled all model information. AdV, IM, RS, and LS compiled the sea ice dataset, and IM produced the dataset map. DS co-planned some of the model analysis. MK, and all other here unnamed authors contributed model data. Ds, DF, CB, and JS provide sea ice modelling advice. All authors read the draft and commented on the text.

Competing interests. The authors declare that they have no competing financial interests

https://doi.org/10.5194/cp-2019-165
Preprint. Discussion started: 23 January 2020

Acknowledgements. We acknowledge the QUIGS (Quaternary Interglacials working group endorsed by PAGES and PMIP) for making this comparison possible, in particular thanks to the workshop organised by this groups in Cambridge, UK, in July 2019. We are grateful to the World Climate Research Programme, which, through its Working Group on Coupled Modelling, coordinated and promoted CMIP6. We thank the climate modeling groups for producing and making available their model output, the Earth System Grid Federation (ESGF) for archiving the data and providing access, and the multiple funding agencies who support CMIP6 and ESGF. The Paleoclimate Modelling Intercomparison Project is thanked for coordinating the lig127k protocol and making the model-model and model-data comparisons possible within CMIP6. PMIP is endorsed by WCRP and CLIVAR. We also acknowledge NOAA/OAR/ESRL PSD, Boulder, Colorado, USA for their optimally interpolated sea-ice product, downloaded from their web site at https://www.esrl.noaa.gov/psd/. LS acknowledges support through NE/P013279/1, NE/P009271/1, and EU-TiPES. The project has received funding from the European Union's Horizon 2020 research and innovation programme under grant agreement No 820970. DS and MG acknowledges support from NERC research grant NE/P013279/1. MK is funded by CNRS and MS by a scholarship from CEA and "Convention des Services Climatiques" from IPSL (https://cse.ipsl.fr/). QZ acknowledges the HPC resources provided by the Swedish National Infrastructure for Computing (SNIC) at the National Supercomputer Centre (NSC). LM acknowledges support from the Australian Research Council FT180100606.

https://doi.org/10.5194/cp-2019-165
Preprint. Discussion started: 23 January 2020

Climate of the Past Discussions
Open Access
EGU

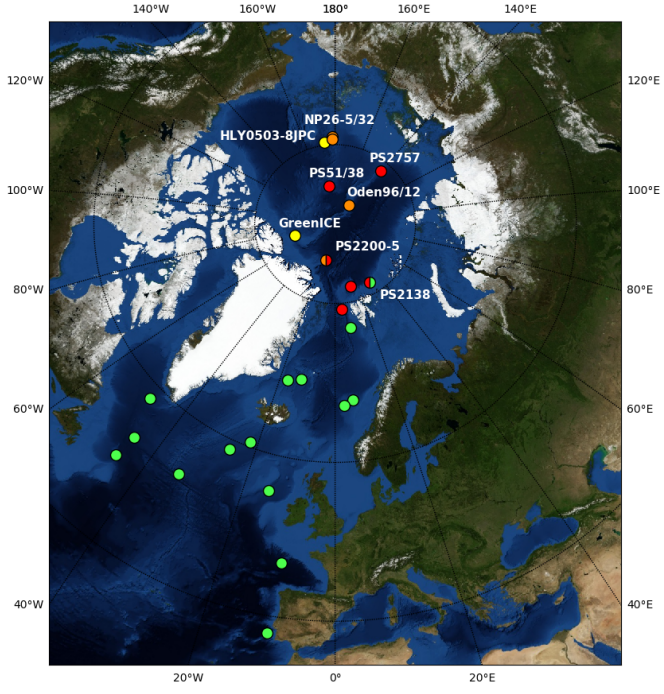

Figure 1. Map showing the location of LIG Arctic cores in Table 1. The map background has been created using http://visibleearth.nasa.gov.

https://doi.org/10.5194/cp-2019-165
Preprint. Discussion started: 23 January 2020

Climate of the Past Discussions
Open Access
EGU

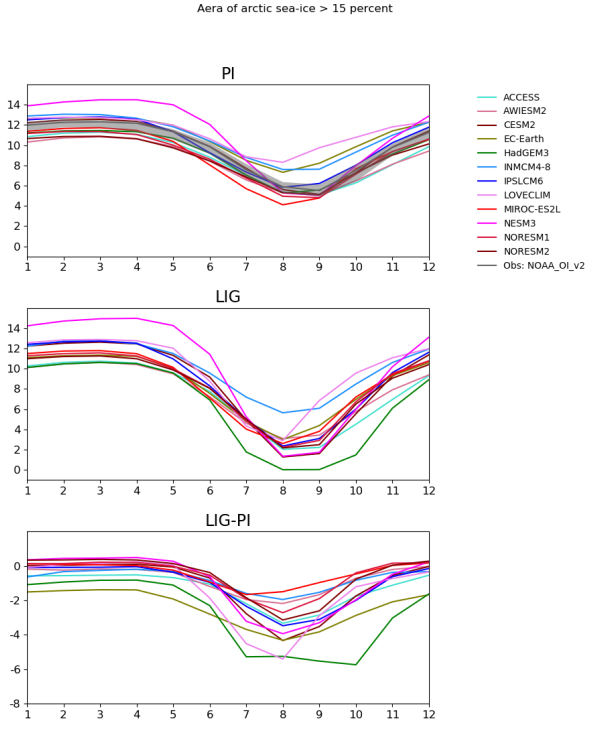

Figure 2. Mean seasonal cycle of the Arctic sea-ice extent simulated for the PI (top) and LIG (middle) simulations, and Arctic sea-ice extent LIG – PI anomaly (bottom), in $10^6 km^2$. The area shown is that for sea-ice concentrations larger than 0.15. The grey shading shows the monthly minimum/maximum observed sea-ice concentration above 0.15 over the years 1982–2001, as given by the NOAA_OI_v2 data set.

https://doi.org/10.5194/cp-2019-165
Preprint. Discussion started: 23 January 2020

Climate of the Past Discussions

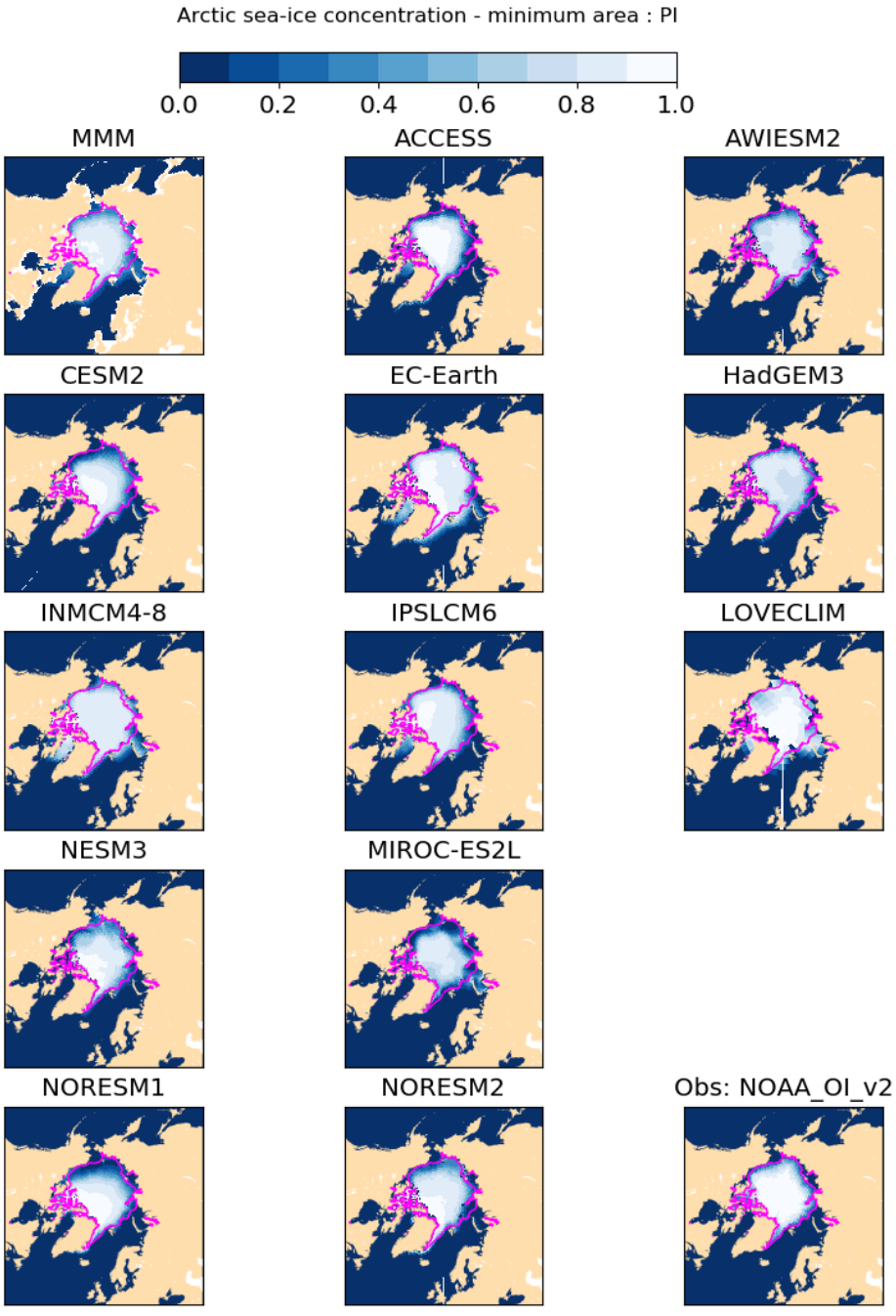

Figure 3. PI sea-ice concentration for the month of minimum extent as computed for Figure 2. The magenta contour shows the 0.15 isocontour of the observations averaged over years 1982–2001.

https://doi.org/10.5194/cp-2019-165
Preprint. Discussion started: 23 January 2020

Climate of the Past Discussions
Open Access
EGU

Figure 4. LIG sea-ice concentration for the month of minimum extent as computed for Figure 2. The magenta contour shows the 0.15 isocontour of the corresponding PI simulation.

https://doi.org/10.5194/cp-2019-165
Preprint. Discussion started: 23 January 2020

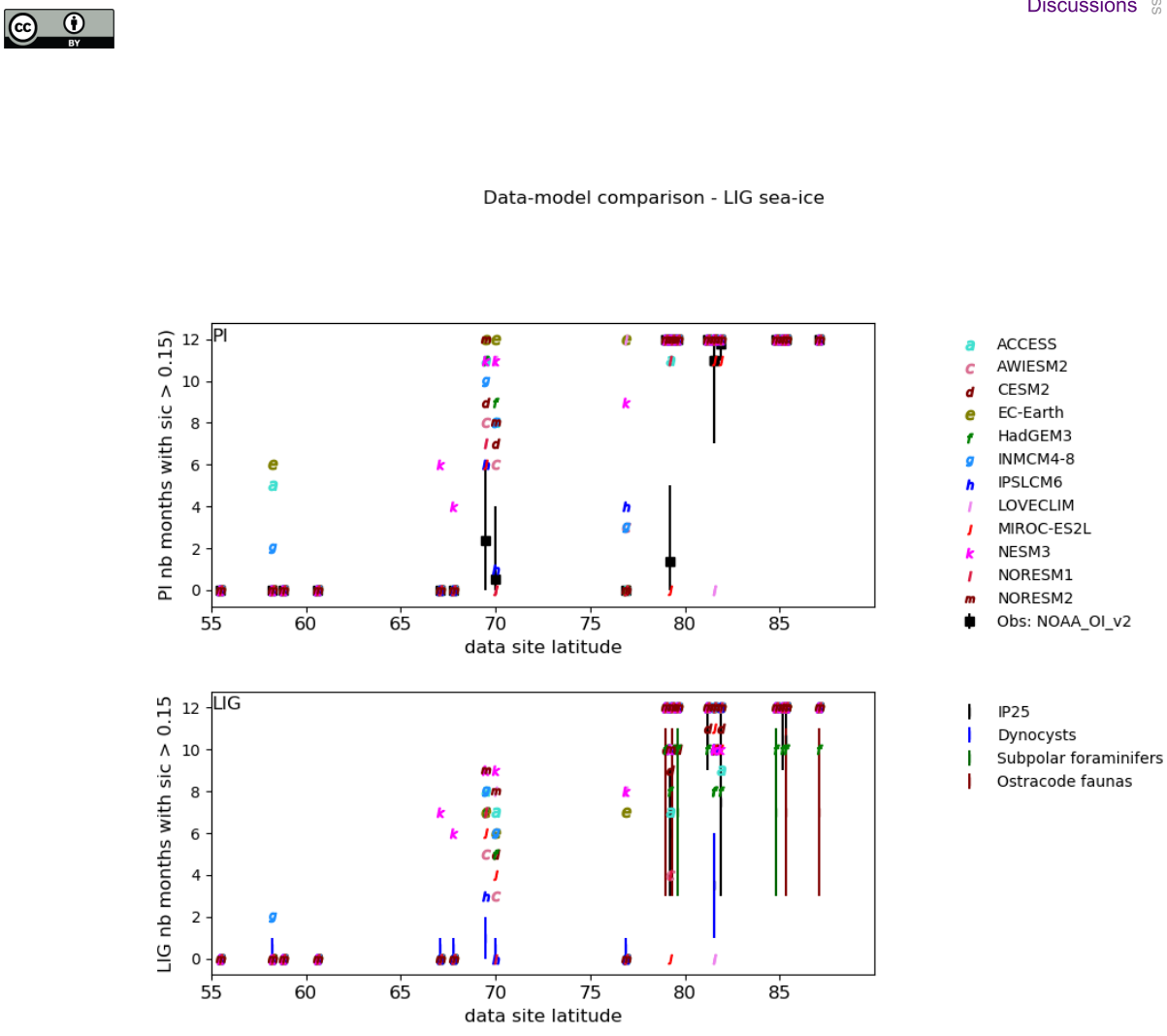

Figure 5. Model-data comparison as a function of latitude for PI and LIG. The model results are shown in terms of number of months of sea-ice fraction > 0.15 in an average year at each data site. For the PI, the values of the NOAA_OI_v2 data sets at the data sites are shown as black squares, with error bars indicating interannual variability over years 1982–2001. For the LIG, the reconstructed minimum and maximum number of months of sea-ice coverage are given as vertical lines.

https://doi.org/10.5194/cp-2019-165
Preprint. Discussion started: 23 January 2020

Climate of the Past
Discussions
Open Access
EGU

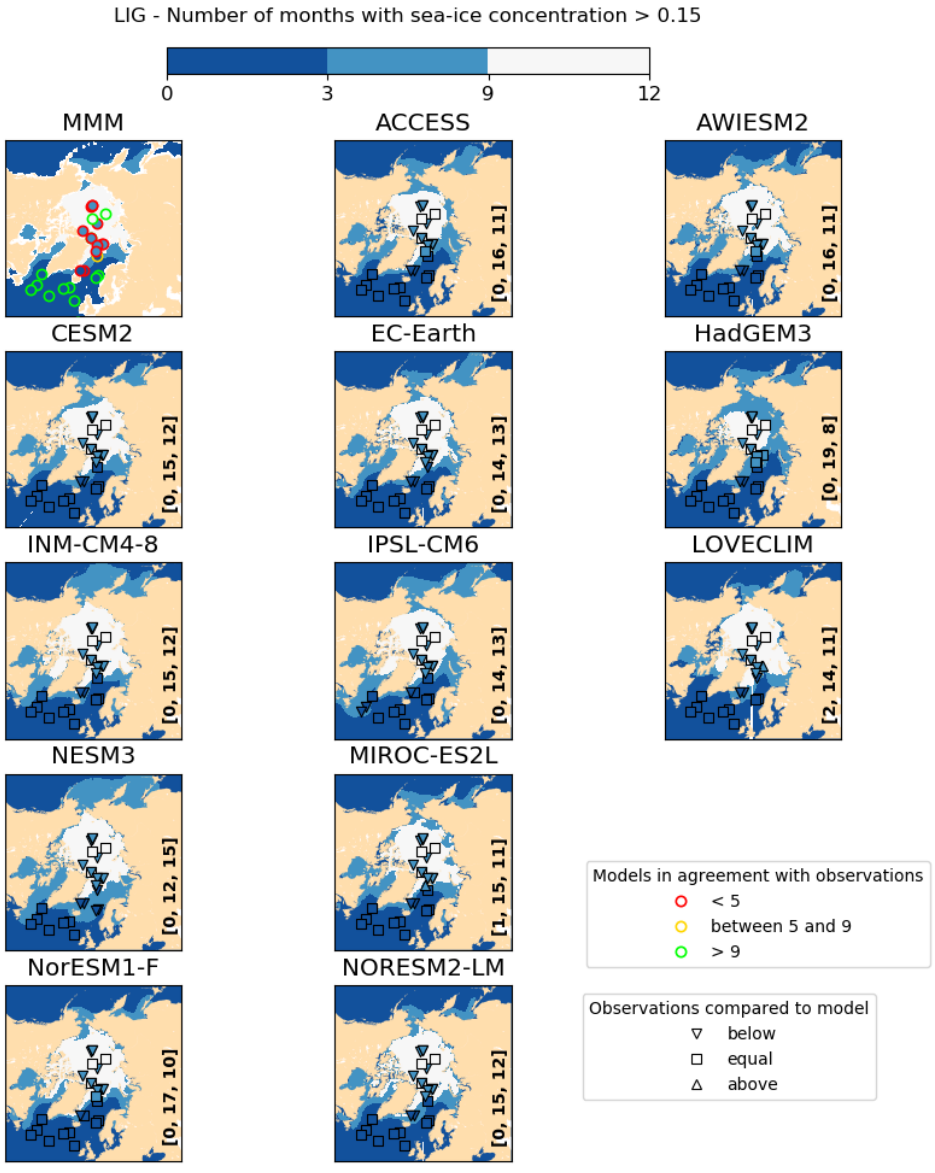

Figure 6. Number of months for which the sea-ice fraction is larger than 0.15, for the multi-model mean (MMM) and for each model, for the LIG. The color filling of the symbols on the maps correspond to the reconstructed values, classified into 3 categories: perennial cover (9 to 12 months), seasonal cover (3 to 9 months), ice free state (0 to 3 months). On the MMM panel, for each data site, the color of the symbol outline corresponds to the number of models simulating the reconstructed ice cover. On the panels for individual models, the shape of the symbol depends on the model result being below the reconstructed one (triangle down), above the reconstructed one (triangle up) or in the same category as the reconstructed one (circle). The number of data points which are above, equal and below the number of months simulated by models are written in the bottom right corner of each panel.

https://doi.org/10.5194/cp-2019-165
Preprint. Discussion started: 23 January 2020

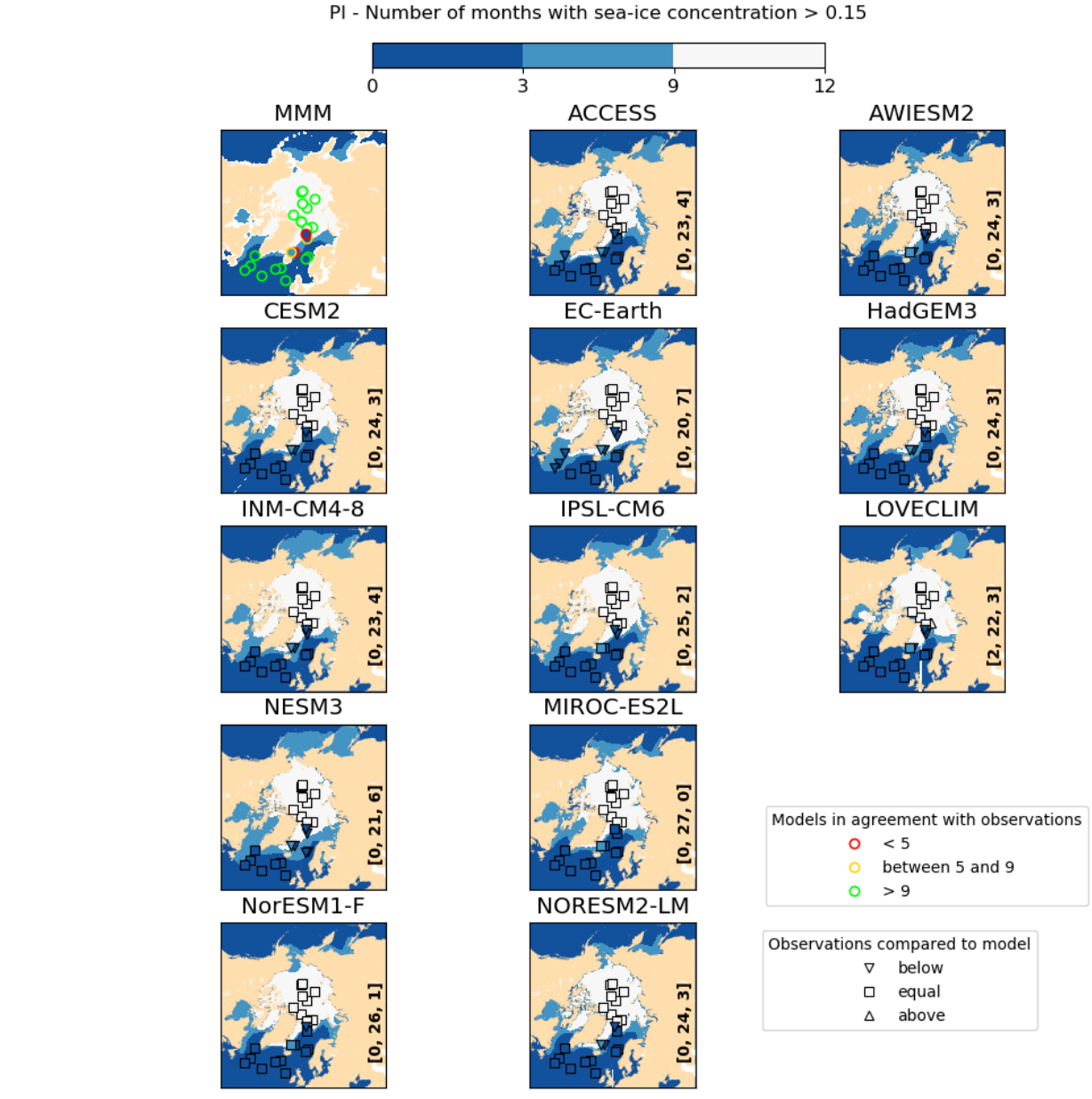

Figure 7. Same as LIG figure for PI, using NOAA_OI_v2 data sets.

https://doi.org/10.5194/cp-2019-165
Preprint. Discussion started: 23 January 2020

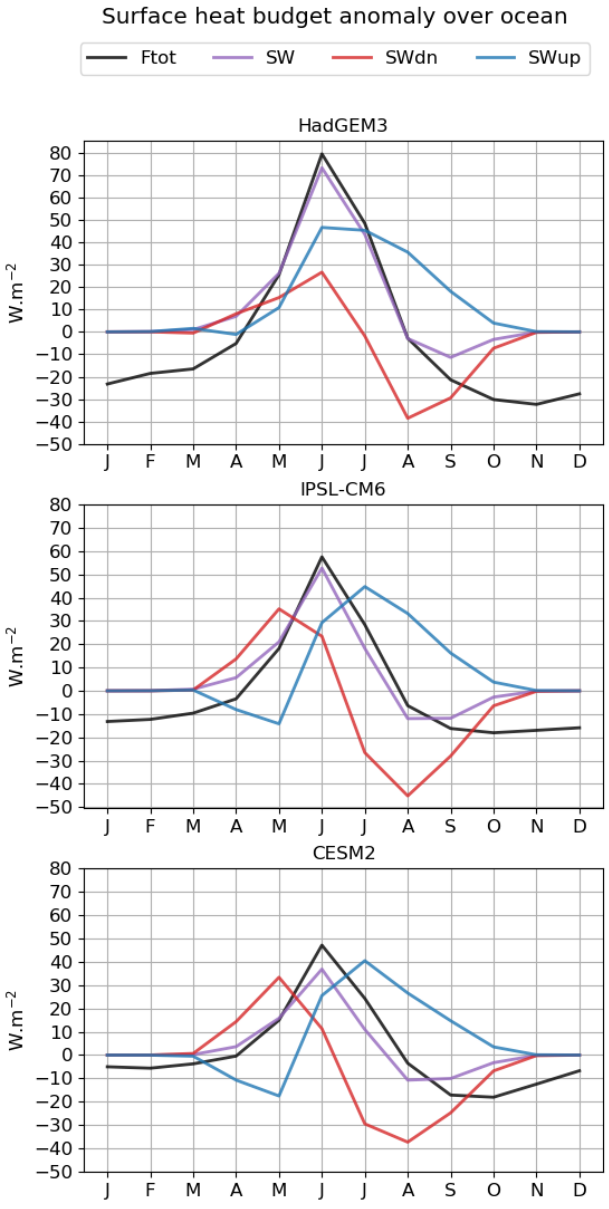

Figure 8. Main components of the atmospheric energy budget averaged over the Arctic for HadGEM3, CESM2 and IPSLCM6. The LIG–PI anomalies as shown as a function of the month for the total energy budget , counted positive downwards (black), the SW budget (violet), and for the downward (red) and upward SW (blue) fluxes, all counted positive downward.

https://doi.org/10.5194/cp-2019-165
Preprint. Discussion started: 23 January 2020

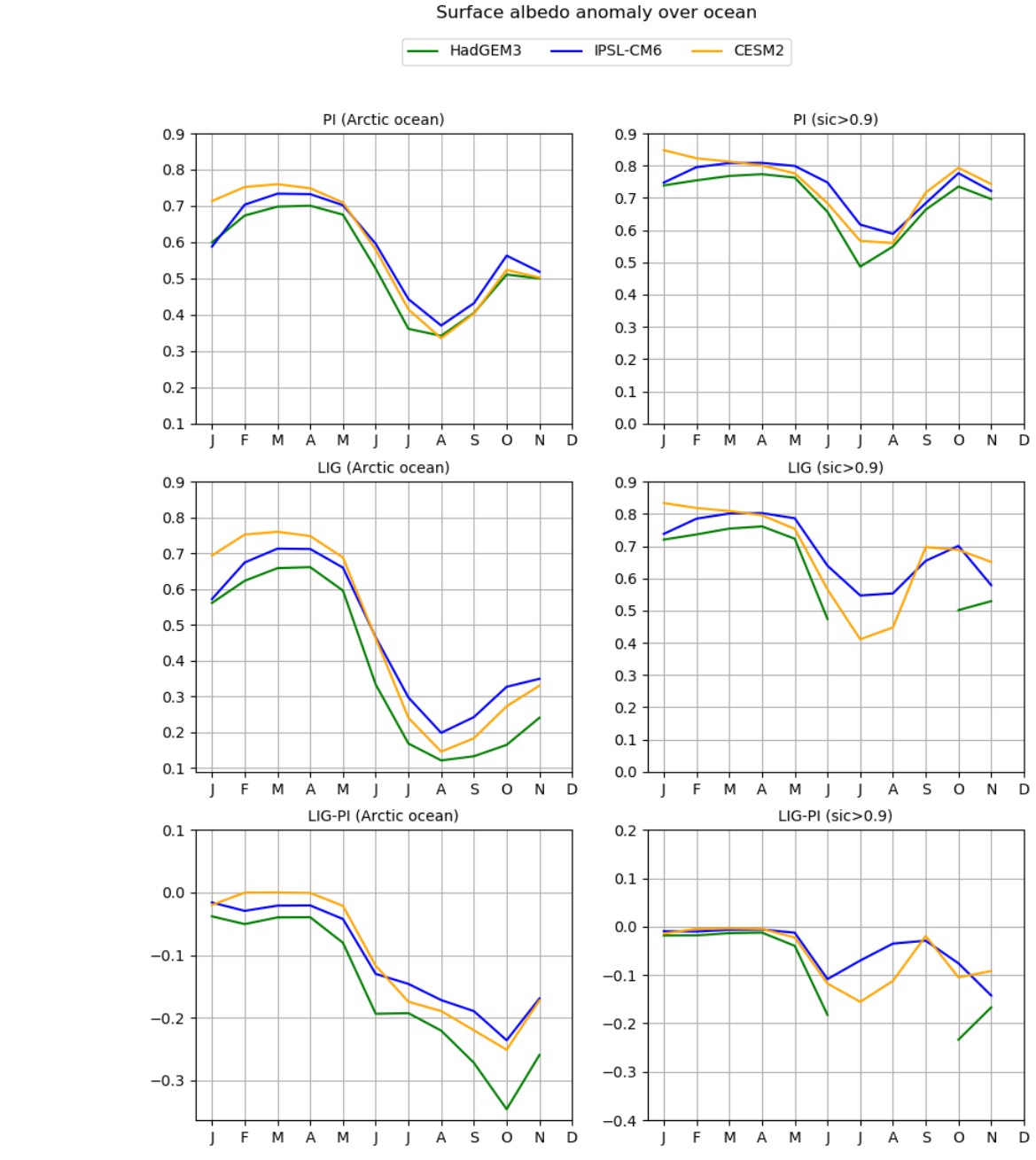

Figure 9. Albedo over the Arctic for PI (top), LIG (middle) and LIG–PI (bottom) for HadGEM3, IPSL-CM6 and CESM2. The albedo has been recomputed from the SWup and SWdn fluxes. The l.h.s. column shows the resuls for the whole Arctic, while the r.h.s. column shows the results for areas where the sea ice fraction is larger than 0.9.

https://doi.org/10.5194/cp-2019-165
Preprint. Discussion started: 23 January 2020

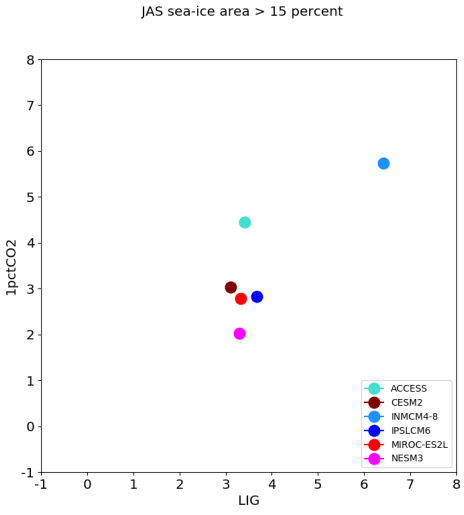

Figure 10. LIG vs 1pctCO2 July-August-September sea ice areas (for sea ice concentrations larger than 0.15). The results for the 1pctCO2 simulations have been averaged for years 50 to 70.

https://doi.org/10.5194/cp-2019-165
Preprint. Discussion started: 23 January 2020

References

Adler, R. E., Polyak, L., Ortiz, J. D., Kaufman, D. S., Channell, J. E. T., Xuan, C., Grottoli, A. G., Selln, E., and Crawford, K. A.: Sediment record from the western Arctic Ocean with an improved Late Quaternary age resolution: HOTRAX core HLY0503-8JPC, Mendeleev Ridge, Global and Planetary Change, 68, 18–29, https://doi.org/10.1016/j.gloplacha.2009.03.026, 2009.

Auclair, G. and Tremblay, L. B.: The role of ocean heat transport in rapid sea ice declines in the Community Earth System Model Large Ensemble., Journal of Geophysical Research: Oceans, 123, 8941–8957, https://doi.org/https://doi.org/10.1029/2018JC014525, 2018.

Bauch, N. V. H. A. and Andruleit, H.: Multiproxy fossil comparison reveals contrasting surface ocean conditions in the western Iceland Sea for the last two interglacials, Palaeogeography, Palaeoclimatology, Palaeoecology, 370, 247–259, https://doi.org/https://doi.org/10.1016/j.palaeo.2012.12.018, 2013.

Belt, S.: Source-specific biomarkers as proxies for Arctic and Antarctic sea ice, Org. Geochem., 125, 277–298, https://doi.org/10.1016/j.orggeochem.2018.10.002, 2018.

Berger, A. and Loutre, M.-F.: Insolation values for the climate of the last 10 million years, Quaternary Science Reviews, 10, 297–317, 1991.

Boucher, O., Servonnat, J., Albright, A. L., Aumont, O., Balkanski, Y., Bastrikov, V., Bekki, S., Bonnet, R., Bony, S., Bopp, L., Braconnot, P., Brockmann, P., Cadule, P., Caubel, A., Cheruy, F., Cozic, A., Cugnet, D., D'Andrea, F., Davini, P., de Lavergne, C., Denvil, S., Dupont, E., Deshayes, J., Devilliers, M., Ducharne, A., Dufresne, J.-L., Ethé, C., Fairhead, L., Falletti, L., Foujols, M.-A., Gardoll, S., Gastineau, G., Ghattas, J., Grandpeix, J.-Y., Guenet, B., Guez, L., Guilyardi, E., Guimberteau, M., Hauglustaine, D., Hourdin, F., Idelkadi, A., Joussaume, S., Kageyama, M., Khadre-Traoré, A., Khodri, M., Krinner, G., Lebas, N., Levavasseur, G., Lévy, C., Lott, F., Lurton, T., Luyssaert, S., Madec, G., Madeleine, J.-B., Maignan, F., Marchand, M., Marti, O., Mellul, L., Meurdesoif, Y., Mignot, J., Musat, I., Ottlé, C., Peylin, P., Planton, Y., Polcher, J., Rio, C., Rousset, C., Sepulchre, P., Sima, A., Swingedouw, D., Thiéblemont, R., Vancoppenolle, M., Vial, J., Vialard, J., Viovy, N., and Vuichard, N.: Presentation and evaluation of the IPSL-CM6A-LR climate model, Journal of Advances in Modeling Earth Systems, submitted, 2019.

Brigham-Grette, J. and Hopkins, D. M.: Emergent marine record and paleoclimate of the last interglaciation along the northwest Alaskan coast, Quaternary Research, 43, 159–173, https://doi.org/10.1006/qres.1995.1017, 1995.

Cao, J., Wang, B., Yang, Y.-M., Ma, L., Li, J., Sun, B., Bao, Y., He, J., Zhou, X., and Wu, L.: The NUIST Earth System Model (NESM) version 3: description and preliminary evaluation, Geoscientific Model Development, 11, 2975–2993, https://doi.org/10.5194/gmd-11-2975-2018, https://www.geosci-model-dev.net/11/2975/2018/, 2018.

Capron, E., Govin, A., Feng, R., Otto-Bliesner, B. L., and Wolff, E. W.: Critical evaluation of climate syntheses to benchmark CMIP6/PMIP4 127 ka Last Interglacial simulations in the high-latitude regions, Quaternary Science Reviews, 168, 137–150, https://doi.org/10.1016/j.quascirev.2017.04.019, 2017.

Cronin, T., Gemery, L., Briggs Jr., W. M., Jakobsson, M., Polyak, L., and Brouwers, E.: Quaternary Sea-ice history in the Arctic Ocean based on a new Ostracode sea-ice proxy, Quat. Sci. Rev., 29, 3415–3429, https://doi.org/10.1016/j.quascirev.2010.05.024, 2010.

Danabasoglu, G., Lamarque, J. F., Bachmeister, J., Bailey, D. A., DuVivier, A. K., Edwards, J., Emmons, L. K., Fasullo, J., Garcia, R., Gettelman, A., Hannay, C., Holland, M. M., et al.: The Community Earth System Model version 2 (CESM2), Journal of Advances in Modeling Earth Systems, submitted, 2019.

de Vernal, A. and Hillaire-Marcel, C.: Natural Variability of Greenland Climate, Vegetation and Ice Volume during the Last Million Years, Science, 320, 1622–1625, https://doi.org/https://doi.org/10.1126/science.1153929, 2008.

https://doi.org/10.5194/cp-2019-165
Preprint. Discussion started: 23 January 2020

de Vernal, A., Eynaud, F., Henry, M., Hillaire-Marcel, C., Londeix, L., Mangin, S., Matthiessen, J., Marret, F., Radi, T., Rochon, A., Solignac, S., and Turon, J.-L.: Reconstruction of sea-surface conditions at middle to high latitudes of the Northern Hemisphere, https://doi.org/10.1594/PANGAEA.738562, https://doi.org/10.1594/PANGAEA.738562, supplement to: de Vernal, A et al. (2005): Reconstruction of sea-surface conditions at middle to highlatitudes of the Northern Hemisphere during the Last Glacial Maximum(LGM) based on dinoflagellate cyst assemblages. Quaternary Science Reviews, 24(7-9), 897-924, https://doi.org/10.1016/j.quascirev.2004.06.014, 2005.

de Vernal, A., Hillaire-Marcel, C., and Darby, D. A.: Variability of sea ice cover in the Chukchi Sea (western Arctic Ocean) during the Holocene, Paleoceanography, 20, https://doi.org/https://doi.org/10.1029/2005PA001157, 2005b.

de Vernal, A., Gersonde, R., Goosse, H., Seidenkrantz, M.-S., and W.Wolff, E.: Sea ice in the paleoclimate system: the challenge of reconstructing sea ice from proxies – an introduction, Quaternary Science Reviews, 79, 1–8, https://doi.org/https://doi.org/10.1016/j.quascirev.2013.08.009, 2013a.

de Vernal, A., Rochon, A., Fréchette, B., Henry, M., Radi, T., and Solignac, S.: Reconstructing past sea ice cover of the Northern Hemisphere from dinocyst assemblages: status of the approach, Quaternary Science Reviews, 79, 122–134, https://doi.org/https://doi.org/10.1016/j.quascirev.2013.06.022, 2013b.

de Vernal, A., Radi, T., Zaragosi, S., Nieuwenhove, N. V., Rochon, A., Allana, E., Scheppere, S. D., Eynaud, F., J.Head, M., Limoges, A., Londeix, L., Marret, F., Matthiessen, J., Penaud, A., Pospelova, V., Price, A., and Richerol, T.: Distribution of common modern dinoflagellate cyst taxa in surface sediments of the Northern Hemisphere in relation to environmental parameters: The new n=1968 database, Marine Micropaleontology, https://doi.org/https://doi.org/10.1016/j.marmicro.2019.101796, 2019.

Eynaud, F.: Kystes de Dinoflagellés et Evolution paléoclimatique et paléohydrologique de l'Atlantique Nord au cours du Dernier Cycle Climatique du Quaternaire, Ph.D. thesis, Bordeaux 1 University, 1999.

Eynaud, F., Turon, J., Sánchez-Goñi, M., and Gendreau, S.: Dinoflagellate cyst evidence of 'Heinrich-like events' off Portugal during the Marine Isotopic Stage 5, Marine Micropaleontology, 40, 9–21, https://doi.org/https://doi.org/10.1016/S0377-8398(99)00045-6, 2000.

Eynaud, F., Turon, J., and Duprat, J.: Comparison of the Holocene and Eemian palaeoenvironments in the South Icelandic Basin: dinoflagellate cysts as proxies for the North Atlantic surface circulation, Review of Palaeobotany and Palynology, 128, 55–79, https://doi.org/https://doi.org/10.1016/S0034-6667(03)00112-X, 2004.

Eyring, V., Bony, S., Meehl, G. A., Senior, C. A., Stevens, B., Stouffer, R. J., and Taylor, K. E.: Overview of the Coupled Model Intercomparison Project Phase 6 (CMIP6) experimental design and organization, Geoscientific Model Development (Online), 9, 2016.

Fischer, H., Meissner, K. J., Mix, A. C., Abram, N. J., Austermann, J., Brovkin, V., Capron, E., Colombaroli, D., Daniau, A.-L., Dyez, K. A., et al.: Palaeoclimate constraints on the impact of 2C anthropogenic warming and beyond, Nature geoscience, 11, 474, 2018.

Goosse, H., Brovkin, V., Fichefet, T., Haarsma, R., Huybrechts, P., Jongma, J., Mouchet, A., Selten, F., Barriat, P.-Y., Campin, J.-M., Deleersnijder, E., Driesschaert, E., Goelzer, H., Janssens, I., Loutre, M.-F., Morales Maqueda, M. A., Opsteegh, T., Mathieu, P.-P., Munhoven, G., Pettersson, E. J., Renssen, H., Roche, D. M., Schaeffer, M., Tartinville, B., Timmermann, A., and Weber, S. L.: Description of the Earth system model of intermediate complexity LOVECLIM version 1.2, Geoscientific Model Development, 3, 603–633, https://doi.org/10.5194/gmd-3-603-2010, https://www.geosci-model-dev.net/3/603/2010/, 2010.

Guarino, M.-V., Sime, L. C., Schroeder, D., Lister, G. M. S., and Hatcher, R.: Machine dependence and reproducibility for coupled climate simulations: The HadGEM3-GC3.1 CMIP Preindustrial simulation, Geoscientific Model Development, 2019, 1–25, https://doi.org/10.5194/gmd-2019-83, 2019.

https://doi.org/10.5194/cp-2019-165
Preprint. Discussion started: 23 January 2020

Guo, C., Bentsen, M., Bethke, I., Ilicak, M., Tjiputra, J., Toniazzo, T., Schwinger, J., and Otterå, O. H.: Description and evaluation of NorESM1-F: a fast version of the Norwegian Earth System Model (NorESM), Geoscientific Model Development, 12, 343–362, 2019.

Hajima, T., Watanabe, M., Yamamoto, A., Tatebe, H., Noguchi, M. A., Abe, M., Ohgaito, R., Ito, A., Yamazaki, D., Okajima, H., Ito, A., Takata, K., Ogochi, K., and Watanabe, S.: Description of the MIROC-ES2L Earth system model and evaluation of its climate–biogeochemical processes and feedbacks., Geoscientific Model Development, https://doi.org/https://doi.org/10.5194/gmd-2019-275, https://www.geosci-model-dev-discuss.net/gmd-2019-275/, 2019.

Hazeleger, W., Wang, X., Severijns, C., Ştefănescu, S., Bintanja, R., Sterl, A., Wyser, K., Semmler, T., Yang, S., Van den Hurk, B., et al.: EC-Earth V2. 2: description and validation of a new seamless earth system prediction model, Climate dynamics, 39, 2611–2629, 2012.

He, M., Hu, Y., Chen, N., Wang, D., Huang, J., and Stamnes, K.: High cloud coverage over melted areas dominates the impact of clouds on the albedo feedback in the Arctic., Scientific Reports, 9, 9529, https://doi.org/https://doi.org/10.1038/s41598-019-44155-w, 2019.

Hillaire-Marcel, C., de Vernal, A., Bilodeau, G., and Weaver, A. J.: Absence of deep-water formation in the Labrador Sea during the last interglacial period, Nature, 410, 1073–1077, 2001.

IPCC: Climate Change 2007: The Physical Science Basis. Contribution of Working Group I to the Fourth Assessment Report of the Intergovernmental Panel on Climate Change [Solomon, S., D. Qin, M. Manning, Z. Chen, M. Marquis, K.B. Averyt, M.Tignor and H.L. Miller (eds.)], Tech. Rep. 4, Intergovernmental Panel on Climate Change, Cambridge University Press, Cambridge, United Kingdom and New York, USA., 2007.

IPCC: Climate Change 2013: The Physical Science Basis. Contribution of Working Group I to the Fifth Assessment Report of the Intergovernmental Panel on Climate Change. [Stocker, T.F. and Qin, D and Plattner, G and Tignor, M and Allen, S.K. and Boschung, J and Nauels, A and Xia, Y and Bex, V and Midgley, P.M (eds.)], Tech. Rep. 5, Intergovernmental Panel on Climate Change, Cambridge, United Kingdom and New York, NY, USA, https://doi.org/10.1017/CBO9781107415324, 2013.

Kageyama, M., Braconnot, P., Harrison, S. P., Haywood, A. M., Jungclaus, J. H., Otto-Bliesner, B. L., Peterschmitt, J.-Y., Abe-Ouchi, A., Albani, S., Bartlein, P. J., Brierley, C., Crucifix, M., Dolan, A., Fernandez-Donado, L., Fischer, H., Hopcroft, P. O., Ivanovic, R. F., Lambert, F., Lunt, D. J., Mahowald, N. M., Peltier, W. R., Phipps, S. J., Roche, D. M., Schmidt, G. A., Tarasov, L., Valdes, P. J., Zhang, Q., and Zhou, T.: The PMIP4 contribution to CMIP6 – Part 1: Overview and over-arching analysis plan, Geoscientific Model Development, 11, 1033–1057, https://doi.org/10.5194/gmd-11-1033-2018, https://www.geosci-model-dev.net/11/1033/2018/, 2018.

Kremer, A., Stein, R., Fahl, K., Bauch, H., Mackensen, A., and Niessen, F.: A 190-ka biomarker record revealing interactions between sea ice, Atlantic Water inflow and ice sheet activity in eastern Fram Strait, arktos, 4, https://doi.org/https://doi.org/10.1007/s41063-018-0052-0, 2018a.

Kremer, A., Stein, R., Fahl, K., Ji, Z., Yang, Z., Wiers, S., Matthiessen, J., Forwick, M., Löwemark, L., O'Regan, M., Chen, J., and Snowball, I.: Changes in sea ice cover and ice sheet extent at the Yermak Plateau during the last 160 ka – Reconstructions from biomarker records, Quaternary Science Reviews, 182, 93–108, https://doi.org/https://doi.org/10.1016/j.quascirev.2017.12.016Get rights and content, 2018b.

Lunt *et al.*, D. J.: A multi-model assessment of last interglacial temperatures, Climate of the Past, 9, 699–717, https://doi.org/10.5194/cp-9-699-2013, http://www.clim-past.net/9/699/2013/, 2013.

Malmierca-Vallet, I., Sime, L. C., Valdes, P. J., Capron, E., Vinther, B. M., and Holloway, M. D.: Simulating the Last Interglacial Greenland stable water isotope peak: The role of Arctic sea ice changes, Quaternary Science Reviews, 198, 1–14, https://doi.org/doi.org/10.1016/j.quascirev.2018.07.027, 2018.

https://doi.org/10.5194/cp-2019-165
Preprint. Discussion started: 23 January 2020

Masson-Delmotte, V., Braconnot, P., Hoffmann, G., Jouzel, J., Kageyama, M., L, A., Lejeune, a. Q., Risi, C., Sime, L. C., Sjolte, J., Swingedouw, D., and Vinther, B. M.: Sensitivity of interglacial Greenland temperature and $\delta^{18}O$: ice core data, orbital and increased CO_2 climate simulations, Climate of the Past, 7, 1041–1059, https://doi.org/10.5194/cp-7-1041-2011, 2011.

Matthiessen, J., Knies, J., Nowaczyk, N. R., and Ruediger, S.: Age determination of sediment core PS2138-1, https://doi.org/https://doi.org/10.1594/PANGAEA.728133, supplement to: Matthiessen, J et al. (2001): Late Quaternary dinoflagellate cyst stratigraphy at the Eurasian continental margin, Arctic Ocean: Indications for Atlantic water inflow in the past 150,000 years. Global and Planetary Change, 31(1-4), 65-86, https://doi.org/10.1016/S0921-8181(01)00113-8, 2001.

Nørgaard-Pedersen, N., Mikkelsen, N., Lassen, S. J., Kristoffersena, Y., and Sheldon, E.: Reduced sea ice concentrations in the Arctic Ocean during the last interglacial period revealed by sediment cores off northern Greenland, Paleoceanography, 22, PA1218, https://doi.org/10.1029/2006PA001283, 2007.

Olonscheck, D., Mauritsen, T., and Notz, D.: Arctic sea-ice variability is primarily driven by atmospheric temperature fluctuations., Nature Geoscience, 12, 430–434, https://doi.org/https://doi.org/10.1038/s41561-019-0363-1, 2019.

Otto-Bliesner, B. L., Marshall, S. J., Overpeck, J. T., Miller, G. H., Hu, A., and CAPE Last Interglacial Project members: Simulating Arctic Climate Warmth and Icefield Retreat in the Last Interglaciation, Science, 311, 1751–1753, https://doi.org/10.1126/science.1120808, 2006.

Otto-Bliesner, B. L., Rosenbloom, N., Stone, E. J., McKay, N. P., Lunt, D. J., Brady, E. C., and Overpeck, J. T.: How warm was the last interglacial? New model–data comparisons, Philosophical Transactions of the Royal Society of London A: Mathematical, Physical and Engineering Sciences, 371, 20130 097+, https://doi.org/10.1098/rsta.2013.0097, http://dx.doi.org/10.1098/rsta.2013.0097, 2013.

Otto-Bliesner, B. L., Braconnot, P., Harrison, S. P., Lunt, D. J., Abe-Ouchi, A., Albani, S., Bartlein, P. J., Capron, E., Carlson, A. E., Dutton, A., et al.: The PMIP4 contribution to CMIP6–Part 2: Two interglacials, scientific objective and experimental design for Holocene and Last Interglacial simulations, Geoscientific Model Development, 10, 3979–4003, 2017.

Penaud, A., Eynaud, F., Turon, J., Zaragosi, S., Marret, F., and Bourillet, J.: Interglacial variability (MIS 5 and MIS 7) and dinoflagellate cyst assemblages in the Bay of Biscay (North Atlantic), Marine Micropaleontology, 68, 136–155, https://doi.org/https://doi.org/10.1016/j.marmicro.2008.01.007, 2008.

Reynolds, R. W., Rayner, N. A. andSmith, T. M., C., S. D., and Wang, W.: An improved in situ and satellite SST analysis for climate., J. Climate, 15, 1609–1625, 2002.

Seland, Ø., Bentsen, M., Olivié, D., Toniazzo, T., Gjermundsen, A., Seland Graff, L., Debernard, J., Kumar Gupta, A., He, Y., Kirkevåg, A., Schwinger, J., Tjiputra, J., Schancke Aas, K., Bethke, I., Fan, Y., Griesfeller, J., Grini, A., Guo, C., Heinze, C., Ilicak, M., Hafsahl Karset, I. H., Landgren, O., Liakka, J., Onsum Moseid, K., Nummelin, A., Spensberger, C., Tang, H., Zhang, Z., Iverson, T., and Schulz, M.: The Norwegian Earth System Model, NorESM2 - Evaluation of the CMIP6 DECK and historical simulations, Geoscientific Model Development, p. submitted, 2019.

Sidorenko, D., Rackow, T., Jung, T., Semmler, T., Barbi, D., Danilov, S., Dethloff, K., Dorn, W., Fieg, K., Gößling, H. F., et al.: Towards multi-resolution global climate modeling with ECHAM6–FESOM. Part I: model formulation and mean climate, Climate Dynamics, 44, 757–780, 2015.

Sime, L. C., Risi, C., Tindall, J. C., Sjolte, J., Wolff, E. W., Masson-Delmotte, V., and Capron, E.: Warm climate isotopic simulations: what do we learn about interglacial signals in Greenland ice cores?, Quaternary Science Reviews, 67, 59–80, https://doi.org/10.1016/j.quascirev.2013.01.009, http://dx.doi.org/10.1016/j.quascirev.2013.01.009, 2013.

Stein, R., Fahl, K., Gierz, P., Niessen, F., and Lohmann, G.: Arctic Ocean sea ice cover during the penultimate glacial and the last interglacial, Nature communications, 8, https://doi.org/10.1038/s41467-017-00552-1, 2017.

https://doi.org/10.5194/cp-2019-165
Preprint. Discussion started: 23 January 2020

Tatebe, H., Tanaka, Y., Komuro, Y., and Hasumi, H.: Impact of deep ocean mixing on the climatic mean state in the Southern Ocean., Sci. Rep., 8, 14 479, https://doi.org/doi:10.1038/s41598-018-32768-6, 2018.

Van Nieuwenhove, N. and Bauch, H. A.: Last interglacial (MIS 5e) surface water conditions at the Vøring Plateau (Norwegian Sea), based on dinoflagellate cysts, Polar Research, 27, 175–186, https://doi.org/https://doi.org/10.3402/polar.v27i2.6175, 2008.

Van Nieuwenhove, N., Bauch, H. A., and Matthiessen, J.: Last interglacial surface water conditions in the eastern Nordic Seas inferred from dinocyst and foraminiferal assemblages, Marine Micropaleontology, 66, 247–263, https://doi.org/https://doi.org/10.1016/j.marmicro.2007.10.004, 2008.

Van Nieuwenhove, N., Bauch, H. A., Eynaud, F., Kandiano, E., Cortijo, E., and Turon, J.-L.: Evidence for delayed poleward expansion of North Atlantic surface waters during the last interglacial (MIS 5e), Quaternay Science Reviews, 30, 934–946, https://doi.org/https://doi.org/10.1016/j.quascirev.2011.01.013, 2011.

Volodin, E. M., Mortikov, E. V., Kostrykin, S. V., Galin, V. Y., Lykossov, V. N., Gritsun, A. S., Diansky, N. A., Gusev, A. V., Iakovlev, N. G., Shestakova, A. A., et al.: Simulation of the modern climate using the INM-CM48 climate model, Russian Journal of Numerical Analysis and Mathematical Modelling, 33, 367–374, 2018.

Walsh, J. E., Chapman, W. L., and Fetterer, F.: Gridded Monthly Sea Ice Extent and Concentration, 1850 Onward, Version 1, https://doi.org/doi: https://doi.org/10.7265/N5833PZ5, 2016.

Williams, K., Copsey, D., Blockley, E., Bodas-Salcedo, A., Calvert, D., Comer, R., Davis, P., Graham, T., Hewitt, H., Hill, R., et al.: The Met Office global coupled model 3.0 and 3.1 (GC3. 0 and GC3. 1) configurations, Journal of Advances in Modeling Earth Systems, 10, 357–380, 2018.

Ziehn, T., Lenton, A., Law, R. M., Matear, R. J., and Chamberlain, M. A.: The carbon cycle in the Australian Community Climate and Earth System Simulator (ACCESS-ESM1)-Part 2: Historical simulations., Geoscientific Model Development, 10, 2017.